11th International Conference on Fracture Mechanics of Concrete and Concrete Structures
FraMCoS-11
J. M. Chandra Kishen, A. Ramaswamy, S. Ray and R. Vidyasagar (Eds)
https://doi.org/10.21012/FC11.092381

FRACTURE BEHAVIOR AND ITS INFLUENCE ON THE SHEAR CAPACITY OF HIGH-STRENGTH REINFORCED CONCRETE BEAMS WITH RECYCLED CONCRETE AGGREGATE

SOURAV CHAKRABORTY [*], AND KOLLURU V. L. SUBRAMANIAM [†]

* Department of Civil Engineering, Indian Institute of Technology Hyderabad, Hyderabad, India, ce18resch11008@iith.ac.in

[†] Department of Civil Engineering, Indian Institute of Technology Hyderabad, Hyderabad, India, kvls@ce.iith.ac.in

Key words: Dilatant behaviour, Fracture, Recycled aggregate concrete, Shear capacity.

Abstract: The fracture and shear responses of the concrete with natural coarse aggregate (NCA) and recycled coarse aggregate (RCA) are evaluated. There is a 25 % reduction in the compressive strength of concrete proportioned for 50 MPa characteristic strength in replacing NCA with RCA. The corresponding tensile strength is less sensitive, with a 9% decrease. The fracture surface areas created in concrete with NCA and RCA are comparable. The roughness of the crack formed in the tensile fracture is similar for NCA and RCA. Reinforced shear beams made with NCA and RCA exhibit similar cracking and failure modes. There is a higher level of cracking in the reinforced RCA beams. The shear capacities of reinforced NCA and the RCA beams are, however, nominally equal. The failure in shear is produced by the loss of stress transfer across the flexure-shear crack leading to splitting along the crack. Due to the identical roughness of the shear crack, which is primarily formed in tension, concrete with RCA can sustain comparable shear stress transfer as the NCA.

1.0 Introduction

In place of virgin natural aggregate, RCA recovered from demolished concrete constructions is used more frequently. The use of RCA is increasingly promoted to meet the increasing demand for concrete while simultaneously considering the limited available supply of natural aggregate and lessening the environmental impact of producing natural aggregate. It also enables profitable utilization of the construction waste in concrete manufactured with RCA. Design codes have started allowing RCA in concrete to be used in structural concrete [1–3]. RCA replacement levels for natural aggregate are currently constrained and frequently determined by compressive strength. For instance, up to 30% of natural aggregate replacement with RCA is permitted under the Indian Code of Practice.

Due to its effect on strength and durability [4, 5], RCA use in concrete is now restricted to coarse aggregate [6] at a 30–40% replacement level. Because of the attached mortar part, RCA tends to be more porous, which results in greater water absorption. A large volume of water is absorbed by the adhering mortar's pores, which makes concrete harder to work with and less durable [4, 5]. The mechanical characteristics of concrete decline noticeably at high replacement levels [7].

The packing of the concrete near the ITZ zone also varies when the matrix strength changes, which impacts the concrete's tensile and fracture behaviour. More coarse particles begin to break as the concrete's matrix strength

increases, modifying the failure process and potentially affecting the concrete's ductility and fracture properties. With lower compressive strength, the new ITZ is very weak under compressive loading. With increasing compressive strength, old ITZ becomes the weak link under compression. The influence of matrix strength on the compressive strength of RCA concrete has been studied [8], but the effect of matrix strength on the fracture process in RCA has not been explored in the literature. The tensile strength of concrete with RCA also decreases due to three kinds of ITZs (old mortar to the matrix, old mortar to aggregate, and aggregate to matrix) [9–12]. It is demonstrated that the compressive strength is more responsive to replacement levels than the split tensile strength [8, 13].

With RCA replacement, shear strength decreases from 12 to 15% [14–17]. However, some studies have found that the RCA shear strength is similar to that of NCA concrete [18–20]. Depending on the mixing procedure, even an improvement in the shear capacity has been reported in some cases. This creates the need for a detailed study on the shear behavior of RCA concrete.

The relation between the fracture and shear mechanism of the RCA beams for high-strength concrete is yet to be evaluated. Change in the fracture parameters and crack growth mechanism in the fracture are presented in this study. How a fractured surface is formed in NAC and RAC and the correlation between fracture and shear response is studied. This study aims to understand the difference in fracture and shear mechanisms between the NAC and RAC beams.

2.0 Experimental program

Concrete was made using coarse aggregate in two size fractions of 10 and 20 mm. Both natural aggregate derived from crushed stone and RCA aggregate were used in concrete mixtures. Concrete mixtures were proportioned to achieve target mean strengths of 58 MPa using natural aggregate. The natural aggregate was crushed gravel. The specific gravities of the 10-mm and 20-mm size fractions were 2.64 and 2.66, respectively. The water absorption was 0.3% and 0.5%, respectively, for the 10 and 20-mm size fractions of the natural aggregate. The 10 and 20-mm natural aggregate had an impact resistance determined as per Standard [21] of 11.26% and 5.56%, respectively.

The water absorption of the 10-mm size fraction RCA was 6.88%, while it was 2.04% for the 20-mm size fraction. The 10-mm and 20-mm pieces of RCA had specific gravities of 2.34 and 2.47, respectively. The impact resistance of the 10-mm and 20-mm size fractions of the RCA was 25.73% and 13.73%, respectively. The RCA satisfied the requirement for use as aggregate in concrete (IS 383-2016) with a resistance of less than 30%.

Table 1 shows the mass proportions of the mix for the concrete made with normal aggregate. The aggregate masses are shown in the saturated surface dry (SSD) condition. Concrete made with NCA/RCA is called Natural Aggregate Concrete (NAC)/ Recycled Aggregate Concrete (RAC). The compressive strength of concrete made with NCA is called the grade of concrete. The procedure in [24] was used to proportion the concrete for a given strength. The concrete was prepared in a drum mixer. The dry ingredients were mixed for 2 minutes before adding water. The aggregates were used in their oven-dry state, and the extra water needed for absorption to reach the saturated surface dry (SSD) condition was added. The compressive strength of the NAC and the RAC measured from standard 150 mm cubes were 57 MPa to 42.5 MPa, respectively.

Table 1 Mass proportions by mass for 1.0 m^3 of the concrete mixture

Grade of Concrete	Fine Aggregate	20mm Coarse Aggregate	10mm Coarse Aggregate
M50	706	488	488

Fracture Testing

Fracture testing was performed on notched beams tested in flexure under center-point loading. The testing was performed using a servo-hydraulic closed-loop test

machine, according to EN 14651:2005. Prismatic beams 150 mm by 150 mm by 500 mm were used. A 2 mm wide, 25 mm notch was cut using a circular wet saw. The beams were tested throughout 450 mm. The testing was conducted in CMOD control at a prescribed rate of 0.05 mm/min. During the test, a Linear Variable Differential Transformer (LVTD) was attached to a fixed frame outside the beam to measure the deflection.

Shear Testing

Shear testing was performed on reinforced concrete beams with stirrups placed on one half of the beam, ensuring the beams fail under shear. The testing was performed using a servo-hydraulic closed-loop test machine, according to EN 14651:2005. Prismatic beams of 125 mm width, 250 mm depth, and 1000 mm length were cast for testing purposes. During the test, Linear Variable Differential Transformers (LVTD) were attached to fixed frames outside the beam to measure the deflection in the mid-span and near the support. The schematic diagram of the shear beam and photograph of the test setup is shown in Figure 1.

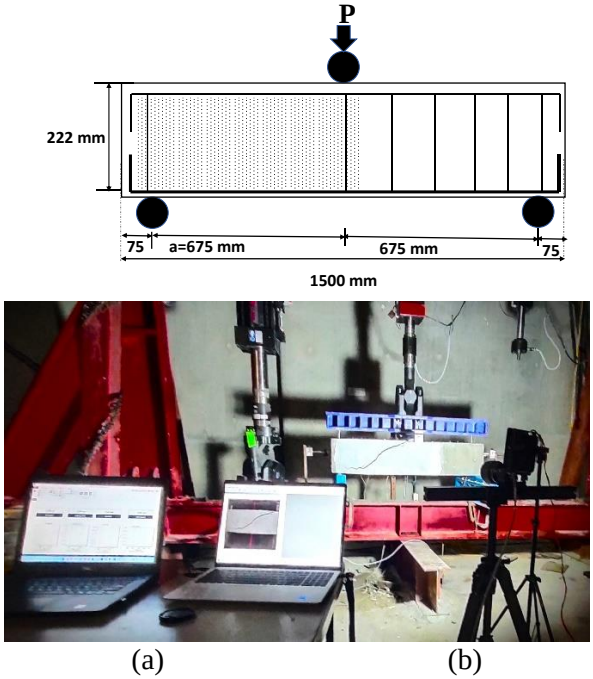

(a) (b)

Figure 1: (a) Details of the shear beam and the loading arrangement (b) Photograph of the test setup

The full-field surface displacement was obtained using the digital image correlation (DIC) method. DIC compares the object's original image with its next image to determine surface displacements. The physical calibration of the photographs was carried out. The measurement's random error was in the range of 0.02 pixels. A "reference image" of the beam in its undeformed state before the load application was captured before the test started. Digital pictures of the specimen were captured throughout the fracture test and saved for later. Cross-correlation analysis was performed on the digital images of the beam specimen captured at different points in the load response. The strain field was calculated as the gradient of the measured displacement field. With the test setup, 1.54 and 7 με were the most conservative estimates for resolutions in the measured displacement and strain [28, 29].

The fracture surface area was measured using a laser-based sensor. The surface area created by fracture was measured over a grid measuring 0.1 by 0.1 millimeters. The surface of the failed beam was scanned at 60 mm/min. Two 50 mm × 50 mm overlapping sections from each beam were scanned.

3.0 Results and Discussions

Fracture responses measured from NAC and RAC beams are presented in Figure 2 (a) as an average of four specimens, and the variations are shown in the scatter bars. The NAC beams have a higher stiffness in the pre-peak part and peak load than the RAC beams. The fracture energy, i.e., the area under the load CMOD curve, is also less for RAC than NAC for any given values of CMOD, as shown in figure 2 (b). The tensile strengths were determined from the fracture test response following an inverse procedure developed previously [30]. The tensile strengths of the NAC and RAC were 3.89 and 3.54 MPa, which results in a 9% reduction.

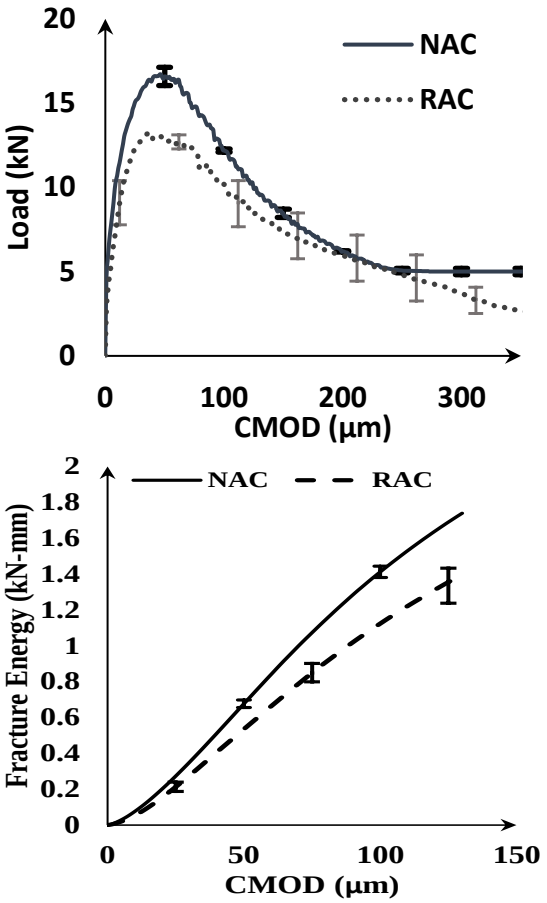

(a)

(b)

Figure 2: (a) Fracture response of NAC and RAC and (b) Variation of fracture energy with increasing CMOD for NAC and RAC.

Figure 3 (a) shows the the fractured surfaces of the of the NAC and RAC beams. In the figure, red-colored shapes are marked to show the aggregates that have been fractured, and black-colored shapes indicate the coarse aggregates that have been pulled out from the matrix. In NAC, some aggregates were cracked, and others were pulled out. For RAC, all the aggregates were cracked. The fracture of all the aggregate in the crack plane contributed to an overall decrease in the fracture energy of concrete made with RCA. Inherently, the RCA are weaker than the NCA, resulting in the fracture plane passing through the RCA. The measurements of the surface areas from the the fractures surfaces of the NAC and RAC beams are shown in Figure 3(b). The normalized area, which is the the total fracture surface area divided by the projected area, was comparable for the concrete made withRCA and NCA. The measurements of the fracture surface areas indicate that the roughness of the crack created in tension is similar for both NAC and RAC.

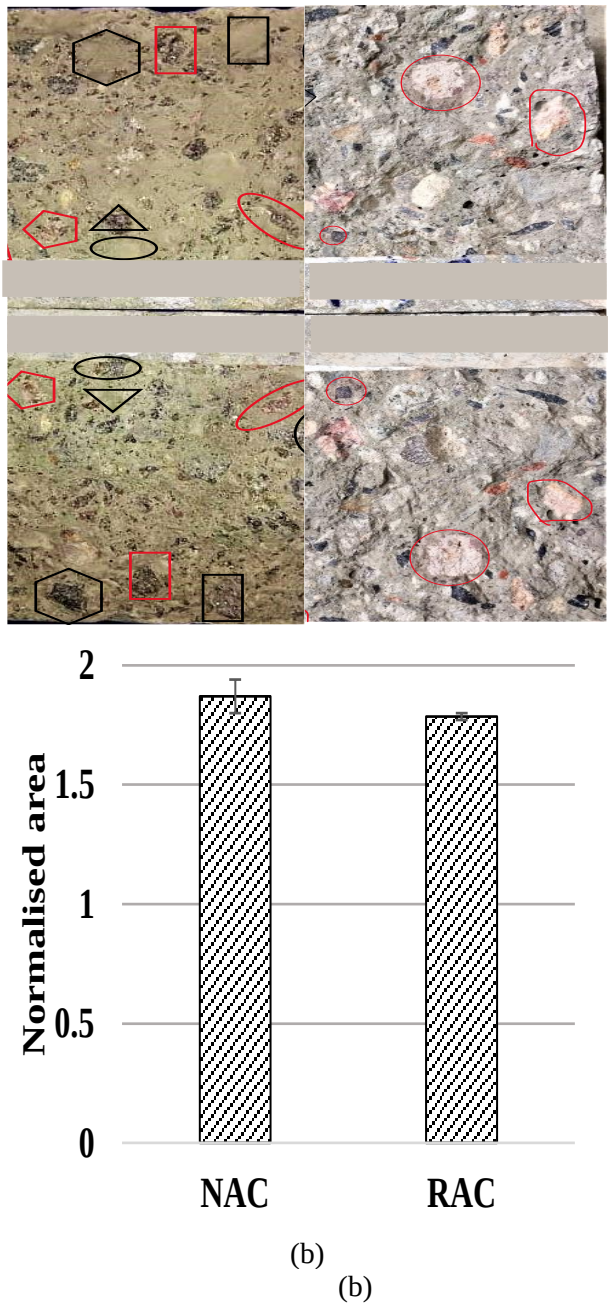

(b)

(b)

Figure 3 (a) Fractured surface of NAC (on the left) and RAC (on the right), (b) Normalised fractured surface area of NAC and RAC.

Shear test responses

Figure 4 (a) and (d) show the load responses from the reinforced concrete beams. The load responses measured from the NAC

and RAC beams are almost similar, with RAC having a marginally lower peak load. Load responses measured from the NAC and RAC beams is essentially linear up to the peak load. The stiffness in the responses of the NAC and RAC beams is also very similar. The failure happened in the 80 to 90 kN range for all the specimens. A shear crack, which extended from the flexural reinforcement at the bottom up to the load point just prior to the peak load. The failure in both NAC and RAC beams was produced immedetialy after the peak load. There was an abrupt loss of load carrying capacity accompanied by visible splitting along the primary shear crack. There was large opening of the shear crack accompanied by a splitting crack that formed and propagated along the flexural rebartowards the support.

Figure 4 (b), (c) and (e), (f) shows the contours of ε_{xx} from the NAC and RAC beams, respectively, at comparable points in the load response. The strain contours help identify the major cracks in the reinforced concrete beam close to the peak load. In both cases, it can be observed that closely-spaced flexure cracks are formed at the bottom of the beam. The crack pattern indicates that one of the flexural cracks at a decreasing angle and propagates as a shear crack close to the neutral axis. At loads of comparable magnitude, the crack patterns indicate that the cracking if further advanced in RAC beams compared to NAC beams. For instance, at load point marked 1, three flexural cracks are clearly identified in NAC beams. The flexure-shear crack is starting to form from the flexure crack located farthest from the load point. At load point 1, a larger number of flexure cracks are seen in the RAC beams. Further, the flexure shear crack has formed from the farthermost flexure crack and it has propagated above the neutral axis. The cracking in shear is parimarily in of tensile nature, broadly forming perpendicular to the principal tensile stress.

At the peak load, the shear crack is fully formed and it extends between the flexural reinforcement and the load point. The crack exhibited curvature and a decreasing angle with respect to the horizontal as it propagated above the neutral axis. After attaining the peak load, the failure was sudden, accompanied by an abrupt opening of the primary shear crack and splitting along the rebar.

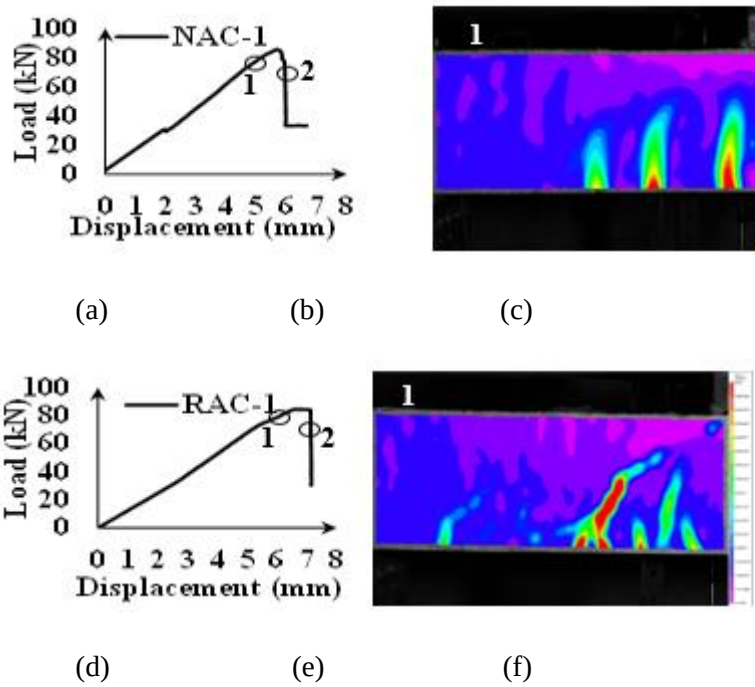

Figure 4: Contours of strain in the X direction of NAC and RAC beams at Points 1 and 2 in the shear response, respectively.

The cracking in the shear response of the reinforced beams is tensile in nature; The tensile stresses determine the direction of propagation of flexure-shear cracks. The observations in the shear cracking can be related with the fracture responses of NAC and RAC. The tensile strength of the RAC from the fracture tests is lower than the NAC. This is reflected in the cracking pattern observed in the reinforced concrete beams. The lower tensile strength of the RAC contributes to more advancement in the cracking in RAC compared to NAC at comparable loads.

Once the shear crack is established, the ultimate shear load capacity is determined by the stress-transfer capacity across the shear crack. The surface characteristics, primarily the fracture surface roughness, determines the stress transfer capacity across the shear crack. RCA produced a comparable fractured surface area as NAC. The fundamental similarity in

the fracture surfaces created in NAC and RAC results in the same shear stress transfer as a function of the crack opening. In RAC, the nature of the crack surface produced is such that it can sustain comparable shear stress transfer as the NAC.

4.0 Conclusions

The analysis of fracture and shear response of NAC and RAC for M50 grade of concrete are presented. Fracture energy, fractured surface area, and crack growth in shear were analysed. The conclusion and the key findings from the study are summarised below.

1. RAC has lower compressive strength than NAC. Complete replacement of NAC with RAC in a concrete matrix proportioned for a characteristic strength of 50 MPa results in a 25% decrease in compressive strength.
2. Pre-peak stiffness and peak load in the fracture are lower for RAC than NAC. The fracture energy of the RAC is also lower. The fracture surface area created in RAC concrete is, however, comparable to the NAC.
3. The loss of stress transfer across the rough shear crack produces shear failure. The shear capacity of the RCA beams is comparable to the NCA beams due to the similar surface area created in NAC and RAC.

5.0 References

1. The International Federation for Structural Concrete (fib) (2011) Model Code 2010
2. IS 456 (2000) Concrete, Plain and Reinforced. Bur Indian Stand Dehli 1–114
3. ACI 318R (2014) ACI 318R-14.pdf
4. Musiket K, Rosendahl M, Xi Y (2016) Fracture of Recycled Aggregate Concrete under High Loading Rates. J Mater Civ Eng 28:04016018. https://doi.org/10.1061/(asce)mt.1943-5533.0001513
5. Dhir RK, de Brito J, Silva R V., Lye CQ (2019) Properties and Composition of Recycled Aggregates
6. Pedro D, De Brito J, Evangelista L (2014) Influence of the use of recycled concrete aggregates from different sources on structural concrete. Constr Build Mater 71:141–151. https://doi.org/10.1016/j.conbuildmat.2014.08.030
7. Kim Y, Hanif A, Kazmi SMS, et al (2018) Properties enhancement of recycled aggregate concrete through pretreatment of coarse aggregates – Comparative assessment of assorted techniques. J Clean Prod 191:339–349. https://doi.org/10.1016/j.jclepro.2018.04.192
8. Biswal US, Dinakar P (2021) A mix design procedure for fly ash and ground granulated blast furnace slag based treated recycled aggregate concrete. Clean Eng Technol 5:100314. https://doi.org/10.1016/j.clet.2021.100314
9. Dilbas H, Şimşek M, Çakır Ö (2014) An investigation on mechanical and physical properties of recycled aggregate concrete (RAC) with and without silica fume. Constr Build Mater 61:50–59. https://doi.org/10.1016/j.conbuildmat.2014.02.057
10. Kou S-C, Zhan B, Poon C-S (2014) Use of a CO2 curing step to improve the properties of concrete prepared with recycled aggregates. Cem Concr Compos 45:22–28. https://doi.org/10.1016/j.cemconcomp.2013.09.008
11. Kou S-C, Poon C-S (2010) Properties of concrete prepared with PVA-impregnated recycled concrete aggregates. Cem Concr Compos 32:649–654. https://doi.org/10.1016/j.cemconcomp.2010.05.003
12. Musiket K, Rosendahl M, Xi Y (2016) Fracture of Recycled Aggregate Concrete under High Loading Rates. J Mater Civ Eng 28:04016018. https://doi.org/10.1061/(ASCE)MT.1943-5533.0001513
13. Savva P, Ioannou S, Oikonomopoulou K, et al (2021) A Mechanical Treatment Method for Recycled Aggregates and Its Effect on Recycled Aggregate-Based Concrete. Materials 14:2186. https://doi.org/10.3390/ma14092186
14. Choi HB, Yi CK, Cho HH, Kang KI (2010) Experimental study on the shear strength of recycled aggregate concrete beams. Mag Concr Res 62:103–114. https://doi.org/10.1680/macr.2008.62.2.103
15. Liu B, Feng C, Deng Z (2019) Shear behavior of three types of recycled aggregate concrete. Constr Build Mater 217:557–572. https://doi.org/10.1016/j.conbuildmat.2019.05.079

16. Xiao J, Xie H, Yang Z (2012) Shear transfer across a crack in recycled aggregate concrete. Cem Concr Res 42:700–709. https://doi.org/10.1016/j.cemconres.2012.02.006
17. Schubert S, Hoffmann C, Leemann A, et al (2012) Recycled aggregate concrete: Experimental shear resistance of slabs without shear reinforcement. Eng Struct 41:490–497. https://doi.org/10.1016/j.engstruct.2012.04.006
18. Ignjatović IS, Marinković SB, Tošić N (2017) Shear behaviour of recycled aggregate concrete beams with and without shear reinforcement. Eng Struct 141:386–401. https://doi.org/10.1016/j.engstruct.2017.03.026
19. Zhang H, Calvi PM, Lehman D, et al (2020) Response of Recycled Coarse Aggregate Concrete Subjected to Pure Shear. J Struct Eng 146:04020075. https://doi.org/10.1061/(ASCE)ST.1943-541X.0002620
20. Fathifazl G, Razaqpur AG, Burkan Isgor O, et al (2011) Shear capacity evaluation of steel reinforced recycled concrete (RRC) beams. Eng Struct 33:1025–1033. https://doi.org/10.1016/j.engstruct.2010.12.025
21. IS 2386-4 (1963): Methods of test for aggregates for concrete, Part 4: Mechanical properties. 37
22. Abdollahnejad Z, Mastali M, Falah M, et al (2019) Construction and Demolition Waste as Recycled Aggregates in Alkali-Activated Concretes. Materials 12:4016. https://doi.org/10.3390/ma12234016
23. Coarse and Fine Aggregate for Concrete - Specification.pdf
24. IS 13920: Ductile Detailing Of Reinforced Concrete Structures Subjected To Seismic Forces - Code Of Practice. 23
25. Chu TC, Ranson WF, Sutton MA (1985) Applications of digital-image-correlation techniques to experimental mechanics. Exp Mech 25:232–244. https://doi.org/10.1007/BF02325092
26. Sutton M, Wolters W, Peters W, et al (1983) Determination of displacements using an improved digital correlation method. Image Vis Comput 1:133–139. https://doi.org/10.1016/0262-8856(83)90064-1
27. Sutton MA, McNeill SR, Jang J, Babai M (1988) Effects Of Subpixel Image Restoration On Digital Correlation Error Estimates. Opt Eng 27:. https://doi.org/10.1117/12.7976778
28. Bruck HA, McNeill SR, Sutton MA, Peters WH (1989) Digital image correlation using Newton-Raphson method of partial differential correction. Exp Mech 29:261–267. https://doi.org/10.1007/BF02321405
29. Schreier HW, Sutton MA (2002) Systematic errors in digital image correlation due to undermatched subset shape functions. Exp Mech 42:303–310. https://doi.org/10.1007/BF02410987
30. Reddy, K.C., Subramaniam, K. V. L. (2017). Analysis for multi-linear 606 stress-crack opening cohesive relationship: Application to macro-synthetic fiber reinforced concrete. Engineering Fracture Mechanics, 169, 128–145. https://doi.org/10.1016/j.engfracmech.2016.11.015